

On-Line Sorting of Wood Treated with Chromated Copper Arsenate Using Laser-Induced Breakdown Spectroscopy

T. M. MOSKAL and D. W. HAHN*

Department of Mechanical Engineering, University of Florida, Gainesville, FL 32611-6300

This paper details the design, implementation, and field evaluation of an online detector system using laser-induced breakdown spectroscopy (LIBS) for the analysis of copper chromated arsenate (CCA) treated wood products. The LIBS-based instrument functioned by creating the laser-induced plasma directly on the sample surface while wood was translated under the detector system, and was successful in discriminating between CCA treated wood and untreated wood products based on the atomic emission signal of chromium. The system was optimized for plasma emission collection both in and out of the laser focal plane and temporally optimized for chromium analysis using a compact, non-intensified charge-coupled device (CCD)/spectrometer unit. Using either single laser pulse spectra or 5-shot and 10-shot spectral averages, the accuracy of LIBS-based analysis ranged from 92 to 100% for identifying both CCA treated and untreated wood samples from the waste stream at a construction and demolition debris recycling center. Additional implementation issues are discussed in the context of LIBS-based on-line sorting of construction and demolition wood debris.

Index Headings: Laser-induced breakdown spectroscopy; Copper chromated arsenate (CCA) treated wood; Chromium.

INTRODUCTION

The commercial introduction of chromated copper arsenate (CCA) in the 1970s as a preservative treatment process was intended to extend the useful service life of wood products by protecting them from insect and fungal deterioration. Since the introduction of CCA, its use has risen to over 70% by volume of all treated wood products sold in 1996, while the volume of CCA treated wood has increased from 248 to 591 million cubic feet.¹ The most significant advantage of CCA treatment is that it has a useful life of at least 25 years, as compared to only a few years for untreated southern pine lumber exposed to the weather. The arsenic in CCA protects the wood from insects while the copper acts as a fungicide. The role of the chromium is to "fix" the copper and arsenic in the wood to maintain an effective chemical concentration for the duration of its useful life. The CCA retention level specified is dependent on the application of the wood. Common retention values are 0.25 pounds of CCA per cubic foot (pcf) of wood for above-ground use, 0.40 pcf for ground/freshwater contact, 0.60 pcf for salt-water splash and wood foundations, and 2.50 pcf for saltwater immersion. The CCA chemical comes in three formulations, with the most common composed of 47.5% CrO_3 , 18.5% CuO , and 34.0% As_2O_5 . Using the average density of southern pine (~ 34 lbs/ft³), the CCA chemical formulation, and the four retention levels, elemental metal concentrations may range from about 1400 to 25 000 ppm for chromium, 1100 to 11 600 ppm for copper, and 800

to 21 600 ppm for arsenic. The average values for CCA treated wood sold in Florida and Georgia in 1996 contained elemental metal concentrations of approximately 3200 ppm chromium, 1900 ppm copper, and 2900 ppm arsenic.²

When used wood products are taken out of service, disposal options include incineration, recycling as landscape mulch, and landfill disposal. Incineration of CCA treated wood is limited by concerns of elevated toxic metal concentrations in the wood ash from biomass combustors,³ while recycling is generally feasible for only a fraction of the total waste stream. Therefore, the primary disposal option is landfill disposal. However, unlike municipal solid waste landfills, construction and demolition debris landfills are typically unlined, allowing rainwater to migrate through the landfill, creating leachate that can potentially contaminate groundwater. Viable approaches to limiting potential migration from unlined landfills include sorting of wood waste streams to segregate CCA treated lumber.⁴ With successful wood sorting, CCA treated wood can then be disposed of properly, although such disposal protocols are still the subject of debate, while untreated wood can be burned for energy or chipped for reuse as landscaping mulch. As such, successful sorting of CCA treated wood from disposal waste streams remains a fundamental step in a number of possible disposal options.

The important characteristics for sorting CCA treated wood are the ability to sort large volumes of wood quickly and accurately at a reasonable cost. One method currently in use at construction and demolition (C&D) facilities is visual sorting.⁵ However, dirty or weathered CCA treated wood can be very difficult to distinguish from untreated wood, and it is unlikely that visual sorting can produce the accuracy necessary for recycling or incineration of untreated wood stocks. Previous research efforts have examined the use of chemical stains, but such methods are generally labor intensive, time consuming, and subject to inaccuracies with weathered and dirty wood.⁶ X-ray fluorescence (XRF) is a candidate for CCA detection that has also been investigated.⁶ While XRF is an accurate analytical technique for this application, issues include detector sampling time, limitations of detector standoff distance, the use of ionizing radiation, and detector cost. An alternative CCA sorting technology is the focus of the current study, namely the use of laser-induced breakdown spectroscopy (LIBS).

Laser-induced breakdown spectroscopy uses pulsed laser light focused onto the sample medium to form a nearly totally ionized gas (plasma) through dielectric breakdown on the surface. The plasma subsequently envelops part of the solid surface, and subsequent observation of

Received 11 March 2002; accepted 21 June 2002.

* Author to whom correspondence should be sent.

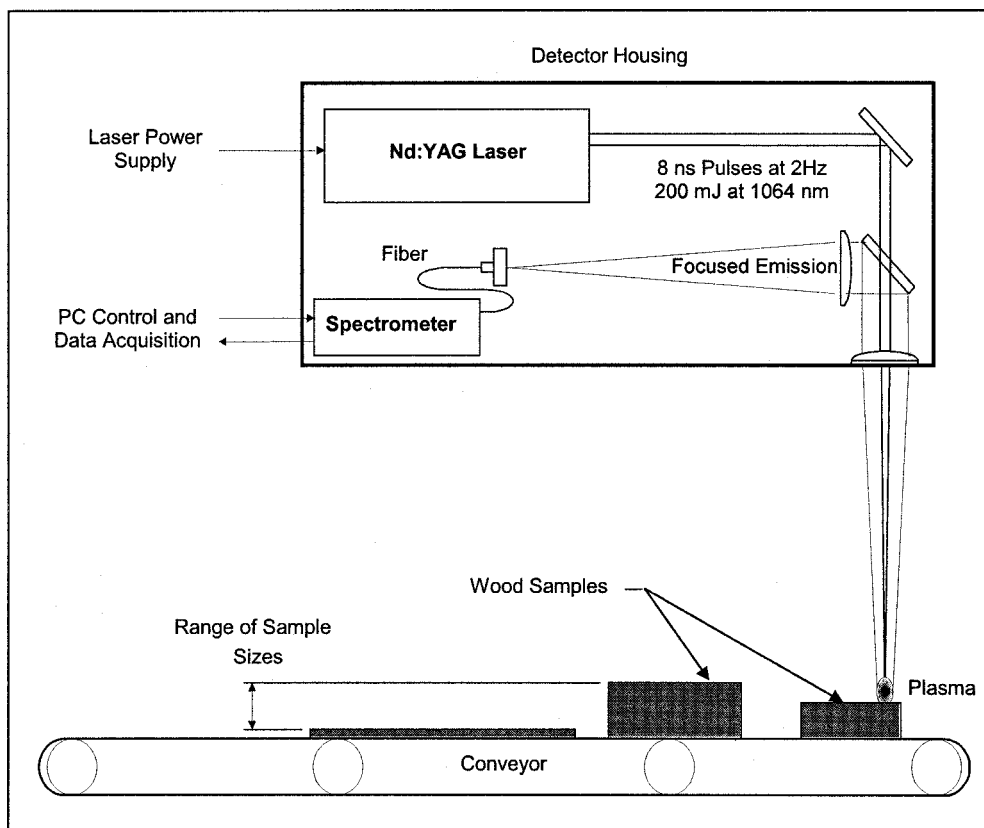


FIG. 1. Schematic of the LIBS detector system.

the resulting plasma emission is the basis of LIBS as an analytical technique. At early times following plasma initiation, the plasma emission is dominated by continuum radiation, primarily recombination and Bremsstrahlung emissions. At longer timescales, ions and neutral species begin to relax back to their ground state, resulting in atomic emission at discrete wavelengths that are unique to each element. LIBS has been applied for *in situ* and real-time analysis as reported in a number of studies. One such application was the use of LIBS for the on-line determination of the elemental composition of encrusted sandstone and stained glass using a KrF excimer laser.⁷ Several research groups have used LIBS for the analysis of toxic metals species, including chromium.⁸⁻¹² In a recent study, researchers used a commercial LIBS system for the analysis of wood preservers.¹³ The bench top system employed an Nd:YAG laser operating at 1064 nm with a 10 Hz repetition rate. While neither elemental arsenic, chromium, nor the CCA chemical were the primary focus of the study, the researchers demonstrated the ability to apply LIBS to the detection of wood preservers, as well as the quantitative analysis of metal concentration levels within the wood samples. Although relatively small wood samples were placed in the instrument for analysis, the authors concluded that LIBS could be applied to wood recycling facilities.

The current study reports on the design and implementation of a field portable LIBS detector system designed for rapid, real-time, *in situ* analysis to discriminate between untreated wood and CCA treated wood in typical construction and demolition debris waste streams.

EXPERIMENTAL METHODS AND INSTRUMENT DESIGN

A Q-switched Nd:YAG laser operating at 1064 nm wavelength, 8 ns pulse width, 2 Hz pulse repetition rate, and 200 mJ pulse energy was used for the LIBS system. The laser beam divergence was 4.1 mrad and the near-field beam diameter was 5.8 mm. A schematic of the layout of the LIBS system is presented in Fig. 1. The laser beam was redirected vertically downward using a dielectric mirror, passed through a 50-mm-diameter pierced broadband mirror, and then focused using a 50-mm-diameter, 200-mm-focal-length plano-convex lens with 1064 nm anti-reflection coating. The long focal length enabled the wood samples to pass underneath the detector housing, while the gradual focus provided an energy density in excess of the breakdown threshold over a relatively broad sample range. Further details of the breakdown threshold are discussed below. The plasma emission was collected axially and collimated by the focusing lens, split off-axis by the broadband pierced mirror, and focused into a 1-mm-diameter multimode fiber optic using a 50-mm, 250-mm-focal-length lens. The 250-mm focal length lens had a broadband anti-reflection coating (355–532 nm) optimized for the relevant plasma emission wavelengths.

The advantage of the axial collection is that while the plasma breakdown can occur at various distances from the focusing lens, the focusing lens will still collect the spectral emission. However, as breakdown occurs on a sample surface that is not positioned at the focal spot,

the plasma emission imaged onto the fiber optic will become defocused, resulting in the collection of less plasma emission. Preliminary results using matched 200-mm focusing lenses for both the plasma collection and focusing to the fiber optic revealed a spatial detection range of less than 50 mm, even though the laser-induced plasma remained intense over a much wider variation in sample position with respect to the focal point. The disadvantage of using a matched 200-mm lens to couple the collection emission to the fiber is a more rapid defocusing if the plasma is not formed at the primary focal point. Matching of these two lenses is a common practice to enhance plasma emission collection for *fixed* sample positions. However, for the current on-line sorting application, wood samples will frequently vary in position with respect to the exact focal spot due to differences in wood sample thickness; hence, the plasma emission will be defocused to some extent. The use of the 250-mm-focal-length lens produced a longer spot, functioning to enhance plasma emission collection over a broader range of wood sizes. A final design improvement was made to further optimize plasma emission collection. Plasma emission collection is optimal when the sample is located precisely at the laser focal point, primarily because the optimal plasma volume is formed at this point of maximum energy density and because the emission is optimally focused onto the fiber optic. Recognizing this, the fiber optic was moved with respect to the focal point of the 250-mm-focal-length lens, such that the plasma emission was optimally focused onto the fiber when the wood sample was positioned about 50 mm above the laser focal spot. This approach functioned to balance the competing effects of reduced plasma emission as the sample is moved upward from the laser focal spot with enhanced emission collection as the emission is optimally focused onto the fiber optic. This approach produced a relatively constant plasma emission signal over a range of sample positions, as presented below.

Plasma emission was launched into the fiber optic and coupled to a compact, integrated spectrometer and a non-intensified charge-coupled device (CCD) detector array (Ocean Optics, model S2000). The spectrometer had a spectral bandwidth of 325–452 nm, an optical dispersion of 0.06 nm per pixel, and an optical resolution of about 0.4 nm. The spectrometer provided excellent resolution of the three chromium(I) atomic emission lines used for the present study, namely the 425.40, 427.50, and 428.90 nm lines.

The laser-induced plasma process was synchronized with the spectrometer integration and temporally optimized to maximize the chromium atomic emission signal. To accomplish this, a TTL output pulse corresponding to the firing of the laser flash lamp was used to trigger a digital delay generator. The actual laser pulse was fired 41.3 μs following the flash lamp trigger. The delay generator produced an outgoing TTL pulse that was used to trigger the spectrometer, but with an appropriate delay introduced such that the detector integration would be initiated to maximize the chromium atomic emission signal. Optimal temporal integration typically was obtained several microseconds following plasma initiation, and full details of the temporal optimization are presented in the following section. The spectrometer system was char-

acterized by a fixed delay of 17 μs between receipt of the external TTL trigger and initiation of actual signal integration. The additional 17 μs of delay was subsequently added to the delay introduced by the delay generator to produce the correct temporal integration with respect to the incident laser pulse. The integration width for the CCD was fixed at about 5 ms for all experiments, the minimum integration time. Background light was negligible for this integration time, resulting in no signal collection in the absence of plasma emission.

The final design included activation of a suitable output signal to notify the system operators when CCA treated wood was detected. The software was designed to analyze multiple emission signals in real-time using a LabView software program. Specifics of plasma emission signal detection and analysis are discussed below. When the chromium emission signal exceeded a predetermined threshold, a PCMCIA digital output card was programmed to produce a 5V TTL pulse for 2 ms. This output pulse was used to trigger a compact array of strobe lights mounted adjacent to the LIBS system. The resulting strobe flashes provided a readily visible real-time signal to indicate the detection of CCA treated wood.

RESULTS AND DISCUSSION

Breakdown Threshold and Spatial Characterization. The laser-induced breakdown threshold was experimentally determined for various species of untreated wood and CCA treated lumber at varying retention levels. A total of 16 wood product samples were collected, including six CCA treated samples and ten untreated samples. Seven wood species were represented, along with engineered sheet products (plywood, particle board, and panel board) and three CCA retention levels (0.25, 0.4, and 2.5 pcf). Three trials were conducted on each of the samples to determine the laser pulse energy such that at least 50% of the laser pulses induced a breakdown on the wood surface. Breakdown was determined by the strong presence of visible plasma emission and a pronounced shock wave. For all experiments, the wood samples were placed at the focal spot of the laser. The variation of laser pulse energy was accomplished by adjusting the laser flash lamp pump energy. Once the breakdown threshold was determined for a given sample, the actual pulse energy was measured with a volume integrating laser energy meter. The laser spot size at the focal plane was measured using burn paper as well as ablation of ink from a microscope slide. The breakdown laser fluence was calculated using the laser pulse energy and the measured cross-sectional beam area.

The breakdown thresholds are summarized in Table I for the various wood products. The results for all wood types revealed an average fluence of 8.5 mJ/mm^2 as the breakdown threshold with a standard deviation of 1.6 mJ/mm^2 . The average threshold for all untreated wood products was slightly higher at 9.0 mJ/mm^2 with a standard deviation of 1.3 mJ/mm^2 , while the average threshold for the CCA treated wood samples was slightly lower at 7.5 mJ/mm^2 with a standard deviation of 1.3 mJ/mm^2 . It is noted that the wood treated at the 2.5 pcf retention value had a markedly reduced breakdown threshold, namely 4.6 mJ/mm^2 , as compared to all other wood samples. It is

TABLE I. Breakdown fluence for various treated and untreated wood samples.

| Wood sample | Breakdown fluence (mJ/mm ²) | |
|--------------------|--|-----------|
| | Mean | Std. Dev. |
| Ponderosa pine | 10.9 | 1.2 |
| Poplar | 7.8 | 0.6 |
| Red oak | 9.6 | 0.8 |
| Pine 2 × 4 | 9.9 | 0.7 |
| Cedar | 10.1 | 0.1 |
| Cypress | 6.7 | 0.3 |
| Mahogany | 8.2 | 1.6 |
| Plywood | 10.1 | 1.4 |
| Particle board | 8.0 | 0.8 |
| Panel board | 9.0 | 0.2 |
| .25 CCA Pine 2 × 4 | 7.0 | 0.3 |
| .4 CCA Pine 2 × 4 | 8.3 | 0.1 |
| .4 CCA Pine 1 × 6 | 8.9 | 0.3 |
| .4 CCA Pine 1 × 6 | 8.6 | 0.3 |
| .4 CCA Plywood | 7.6 | 0.1 |
| 2.5 CCA Pine 2 × 4 | 4.6 | 0.3 |
| Average | 8.5 | 1.6 |

concluded that the significantly increased metal concentration aids in the formation of the seed electrons due to the partially filled electron shells of metals. The earlier formation of seed electrons enables greater absorption of the laser pulse energy by these free electrons, enhancing the cascade breakdown process and thereby promoting breakdown at a reduced laser fluence. Similar behavior was observed with respect to the effect of weathering on the breakdown fluence, which generally reduced the breakdown threshold. Surface dirt and weathering provide micro-sites to trigger earlier the cascade processes associated with breakdown.

For implementation of an online LIBS detector for CCA sorting, the required minimum breakdown fluence was estimated as the mean threshold for all Table I data plus three standard deviations, namely 13.2 mJ/mm². This value ensures consistent breakdown over a wide variety of wood species and retention levels. This threshold value was then compared to the measured laser fluence as a function of distance from the primary focusing optic to provide an estimate of the spatial region expected to produce a reliable laser-induced plasma. The focused beam diameter was measured as a function of distance for the 200-mm focusing lens using ink on glass slides. The ink was readily ablated by the laser beam, producing a clear demarcation of the beam diameter. The measured laser fluence is presented in Fig. 2 along with the superimposed breakdown threshold. The region of predicted breakdown is approximately 135 mm long and is centered about the 200 mm focal spot of the lens. It is noted, however, that plasma formation (i.e., breakdown) is not a sufficient criterion for the actual *detection* of CCA treated wood products. Therefore, additional experiments were performed to assess the spatial distances over which reliable detection of CCA treated wood samples was realized.

For this study, all analysis was based on the atomic emission of chromium, namely the 425.4, 427.5, and 428.9 nm chromium(I) lines. Copper is amenable to detection with the LIBS technique, but is present in alternative wood treatments such as alkaline copper quat

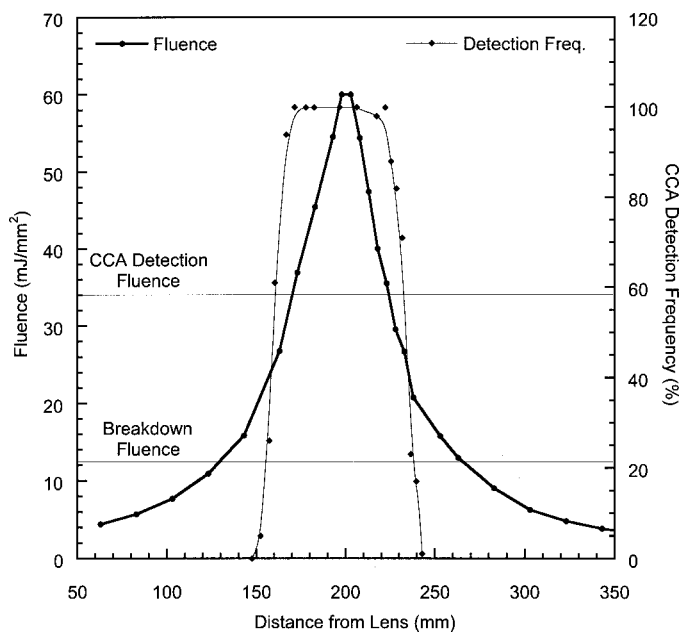


FIG. 2. Profile of the laser beam fluence as a function of distance from the focusing optic ($f = 200$ mm), and the corresponding CCA treated wood detection frequency based on the 425.4 nm chromium emission line. The breakdown fluence and CCA detection fluence are noted.

(ACQ), copper boron azole (CBA), copper citrate (CC), and copper dimethyldithiocarbamate (CDDC). As such, copper is not a unique indicator for CCA treated wood, the target of the present study. Arsenic is unique as an additive to CCA treated wood; however, the most prominent emission lines at 189.0 and 193.8 nm are relatively weak as compared to chromium emission and are situated deep in the UV, making emission collection and detection more difficult.

Measurements were conducted using a pristine (nominally 2 in. × 4 in.) piece of CCA lumber treated at the 0.4 pcf retention level placed at various measured distances from the 200 mm focal plane of the laser beam. For each distance, a number of LIBS spectra were recorded and analyzed using the 425.4 nm chromium atomic emission line. The LIBS signal was quantified using the integrated chromium emission peak area divided by the average plasma continuum emission corresponding to a nearby featureless spectral region. This commonly used peak-to-base ratio eliminates the effect of any variation in the absolute signal strength by normalizing with respect to the continuum, which is important as the absolute signal levels are expected to vary as wood samples vary in distance with respect to the focal plane. The average peak-to-base ratio based on many laser shots was compared for untreated wood samples and for the 0.4 pcf wood sample to determine an appropriate threshold for detection of CCA. Using the threshold value, the single-shot spectra were analyzed for the detection of CCA corresponding to different positions with respect to the focal point of the lens. The CCA detection frequency was calculated as the percentage of laser pulses registering a peak-to-base value above the threshold for the pristine piece of 0.4 pcf treated wood. The wood was translated such that each laser shot was incident on a pristine spot. The detection frequency is plotted in Fig. 2 as a function

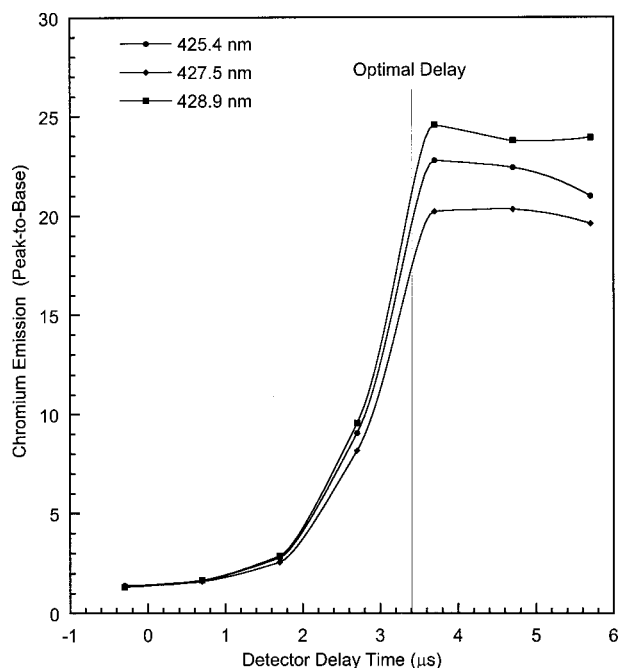


FIG. 3. The chromium atomic emission peak-to-base ratio for the three chromium atomic emission lines as a function of detector signal integration delay with respect to the incident laser pulse.

of distance from the 200 mm focusing lens. As observed in the figure, the detection frequency data reveal a flat region of near 100% frequency centered about the focal point of the lens, with a steep reduction in detection frequency outside of this region. It is noted that the region of nominally 100% CCA detection is narrower than the region characterized by plasma breakdown; hence, plasma formation alone is not a suitable criterion for CCA detection. Extrapolating the envelope of 100% detection frequency to the laser beam fluence profile, a laser fluence threshold for reliable CCA detection is estimated as 34 mJ/mm^2 , which is approximately 2.5 times greater than the breakdown threshold. These values yield a spatial region of about 55 mm over which CCA treated wood samples are expected to be reliably detected based on the chromium emission peak-to-base signal. This 55-mm region is more than adequate to account for the spatial variation expected for the detection of wood samples ranging in thickness from $\frac{1}{4}$ -inch plywood (6 mm) to nominal 2×4 in. boards (44 mm).

Temporal Optimization. As discussed above, temporal gating was used to optimize the chromium emission by taking advantage of the markedly different rates of decay between the continuum emission and chromium atomic emission. To determine the optimal delay, ensemble-averaged spectra from CCA treated wood samples were collected for integration delay times ranging from coincident with the laser pulse to $8 \mu\text{s}$, using $1\text{-}\mu\text{s}$ increments. It is noted that the integration time of the CCD was fixed at 5 ms as discussed above. To quantify the chromium emission, the peak-to-base ratios were calculated for each of the 425.4, 427.5, and 428.9 nm lines using the integrated peak area divided by the baseline continuum intensity using an adjacent, featureless spectral region. The peak-to-base values for all three chromium emission lines are plotted in Fig. 3 as a function

of delay time between the incident laser pulse and the start of signal integration. While both the continuum emission and peak emission intensities decrease with time, the differing rates of decay result in a significant increase in the chromium peak-to-base ratio with increasing delay time. The optimal delay time was determined to be $3.4 \mu\text{s}$ with respect to the incident laser pulse, while it is noted that plasma initiation is essentially coincident with the incident laser pulse. This delay value was used for all subsequent experiments.

An additional benefit is noted with respect to using the peak-to-base ratio as opposed to an *absolute* chromium emission signal, namely signal normalization. With the defocusing effect realized for collected plasma emission due to varying wood sample thickness (i.e., out of focal plane plasma spot), the absolute signal levels fluctuate greatly. However, the plasma continuum emission and atomic emission intensities scale together; hence, the peak-to-base ratios are very consistent and provide an excellent metric for chromium detection.

CCA Detection Threshold Criterion. Field trials were conducted at a construction and demolition (C&D) debris landfill to evaluate the on-line sorting of CCA treated wood products under actual field conditions. Representative samples of both treated and untreated wood were passed under the LIBS system using a roller-type conveyer system. As shown in Fig. 1, the laser was fired downward and positioned such that the laser beam passed between two rollers when no wood was present. With no sample, the divergent laser pulse subsequently struck the concrete floor beneath the conveyer, which functioned as a beam stop. The conveyer speed was set to approximately 5 cm/s, corresponding to about 2.5 cm between laser shots for the 2 Hz pulse rate. Hundreds of single-shot LIBS spectra were recorded for both CCA treated and untreated wood samples. These spectra were then analyzed to calculate the peak-to-base ratio of the 425.4 nm chromium emission peak. The peak-to-base ratios for 450 individual spectra are presented in Figs. 4 and 5 for CCA treated and untreated wood samples, respectively. For both plots, the data were recorded in 25-shot sets for various wood samples, with 25 spectra recorded from both the top and bottom of each sample. Accordingly, the first 25 peak-to-base ratios represent the first surface of a specific wood sample and the next 25 represent the opposite surface of the same sample, with this pattern repeated for different wood samples. Analysis of the single-shot data revealed two key features, namely that the CCA treated wood samples yielded a marked increase in the peak-to-base ratio corresponding to the chromium emission spectral region as compared to the untreated wood samples and that the peak-to-base ratios are characterized by significant signal fluctuations on a shot-to-shot basis. Two representative single-shot spectra are presented in Fig. 6 corresponding to a treated and untreated wood sample. The two chromium peaks are clearly discernable in the CCA treated sample spectrum, as is the pronounced calcium(I) emission peak, present in both samples. As discussed below, the calcium peak may be used to confirm the presence of wood to aid in the discrimination of chromium emission derived from CCA treated wood and possible chromium emission from steel contaminants such as nails and fasteners.

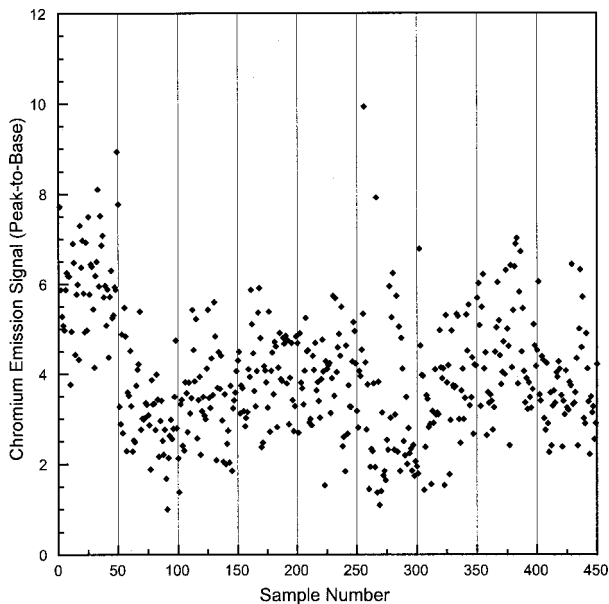


FIG. 4. The single-shot 424.5 nm chromium emission peak-to-base ratios for CCA treated wood samples. Each 50-shot sequence corresponds to 25 individual laser shots on one side of a given wood sample followed by 25 individual laser shots on the opposite sample side.

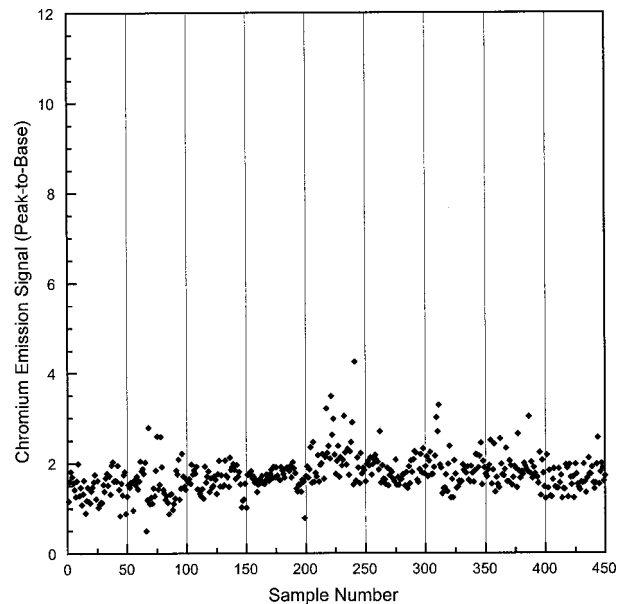


FIG. 5. The single-shot 424.5 nm chromium emission peak-to-base ratios for untreated wood samples. Each 50-shot sequence corresponds to 25 individual laser shots on one side of a given wood sample followed by 25 individual laser shots on the opposite sample side.

The statistical variations of the peak-to-base (P/B) ratios for the data in Figs. 4 and 5 were analyzed to select an appropriate threshold value representative of CCA treated wood. The optimal threshold peak-to-base value for CCA detection is 2.2. The average peak-to-base ratio of all CCA treated wood samples was 3.97 with a standard deviation of 1.39, while the average peak-to-base of the untreated wood samples was 1.74 with a standard deviation of 0.40. The optimal threshold value lies between the mean CCA treated P/B value minus its standard deviation and the mean untreated P/B value plus its standard deviation, as expected. The optimal value was determined to maximize the percentage accuracy of treated and untreated wood identification. Using the P/B threshold value of 2.2 to analyze the 900 single-shot spectra, the CCA treated wood spectra were correctly identified 91.6% of the time, while the untreated sample spectra were correctly identified 95.2% of the time. In practice, it is not necessary to sort wood using a single laser pulse; hence, the above data sets were also analyzed by ensemble-averaging 5 and 10 consecutive single-shot spectra and then calculating the peak-to-base ratio of the resulting spectrum. Using a 5-shot ensemble average per sample increased accuracies to 96.7% for both treated and untreated wood sorting, while a 10-shot analysis perfectly (100%) predicted CCA treated wood, with a corresponding 98.9% accuracy for identification of untreated wood.

CCA Sorting Field Tests. To assess the operation of the LIBS-based system during on-line sorting analysis, additional field tests were performed. Approximately 100 wood samples from the C&D waste stream were fed under the LIBS system. Detection of CCA treated wood was based on the 425.4 nm chromium emission peak-to-base ratio of 2.2, as determined from the above analysis. Each wood sample was exposed to 10 laser pulses (5-s sample period at 2 Hz pulse rate) and the sample was classified as CCA treated if 5 or more of the pulses exceeded the

threshold P/B value. The results are presented in Fig. 7 for 94 sample pieces. Using the criterion of 50% or more of the ten shots for CCA detection, the LIBS system misidentified only two of the 94 wood samples, namely sample numbers 20 and 42, which were CCA treated but were identified as untreated. Of these, sample 20 triggered CCA detection on 4 of the 10 shots, with an average P/B value of 2.28, and sample 42 triggered CCA detection on 3 of the 10 shots, with an average P/B value of 2.08. Hence, both of these samples were marginal misses and would most likely have been correctly identified.

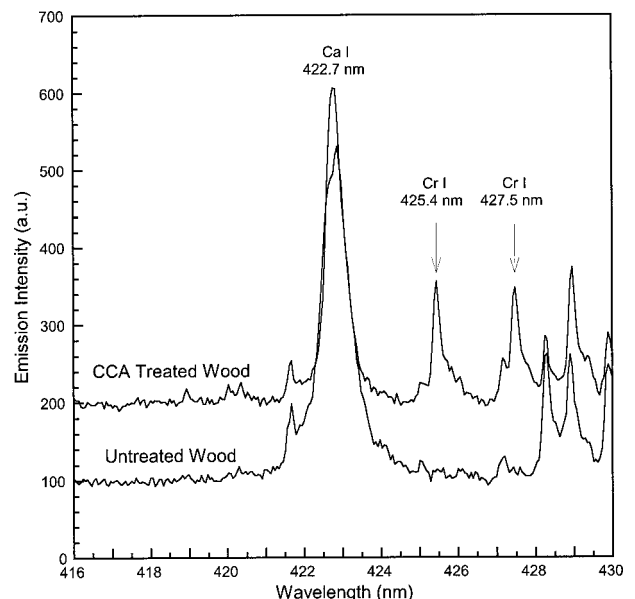


FIG. 6. Single-shot emission spectra corresponding to a typical CCA treated wood sample and an untreated wood sample from a construction and demolition debris waste stream. The CCA treated wood spectrum was shifted up by 100 counts for clarity.

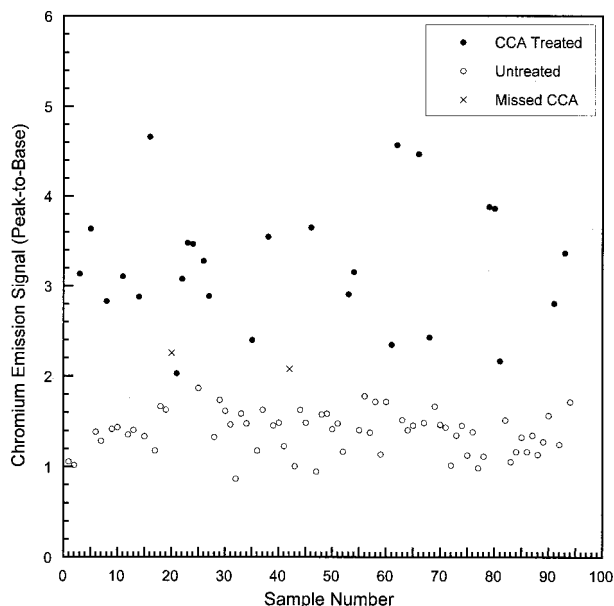


FIG. 7. The LIBS-based analysis results from a field sorting trial of 94 wood samples from a construction and demolition debris waste stream. The CCA treated and untreated samples represent wood samples correctly identified using the LIBS system based on 10 laser shots. The two samples labeled as Missed CCA correspond to actual CCA treated samples that were incorrectly identified by the LIBS system.

tified using a 10-shot ensemble averaged spectrum or a more conservative (i.e., lower) detection threshold. For the 26 correctly identified CCA wood samples, the average number of pulses exceeding the threshold was 8.3 out of 10 with a standard deviation of 1.8. For the 65 correctly identified untreated wood samples, the average number of pulses exceeding the threshold was 0.15 with a standard deviation of 0.5. For these experiments, the strobe lights were set to flash with each laser pulse upon CCA detection, and the strobes were observed independent of known wood type or of the LIBS system analysis. The wood was classified by two observers as treated or untreated based on the same criteria used with LIBS, namely the observation of 5 or more strobe flashes in a ten-shot sequence. The observer results were in perfect agreement with the LIBS analysis as identified through computer output. This data supports the ability of C&D facility workers to sort wood waste streams based on the strobe light outputs in as little as several seconds per sample with the laser operating at 2 Hz. With a laser repetition rate of 10 Hz, which is obtainable with real-time analysis using a faster USB spectrometer interface, the LIBS system could be programmed to provide a strobe output once per second based on an ensemble analysis of every 10 laser shots. Such a scheme could also use the presence of the calcium emission signal to confirm emission from wood surfaces.

Overall, the LIBS system was successful for the detection of a wide range of CCA treated wood products as sampled from a typical C&D wood waste stream. Two notable exceptions are noted. The LIBS system did not prove reliable for the detection of severely rotted wood samples or samples that were completely soaked (i.e., saturated) with water. In both instances, the plasma emission intensity (continuum and atomic emission) was re-

duced significantly from the typical values observed. With such samples, the P/B ratio of the chromium emission peak converged to a nominal value of one, reflecting the lack of a detectable plasma emission signal. The failure to detect such wood samples is due to the poor plasma breakdown conditions of these sample types, presumably due to the dirt-encrusted, poorly defined surface of severely rotted wood samples or the additional heat capacity present with water saturation. The detrimental effects of water content on LIBS-based analysis have been reported previously for CaCO_3 powers.¹⁴ The use of additional laser pulse energy is expected to extend the ability to detect CCA treated wood for these two sample types. It is noted that the use of the 200 mJ per pulse laser resulted in a significant increase in sorting accuracy, notably with damp wood samples, as compared with preliminary experiments using a 50 mJ per pulse laser.

CONCLUSION

The current inventory of CCA treated wood will ultimately require disposal in an environmentally sound manner, commonly in a C&D landfill. Alternatively, wood is a natural candidate for combustion to recover the inherent energy or chipping as mulch to reduce the landfill burden, yet these sources of disposal require the wood stream to be 98 to 100% untreated wood.⁶ To foster a wide range of disposal options, it is desirable to have a system to accurately and quickly sort CCA treated wood from untreated wood. The current study demonstrated that laser-induced breakdown spectroscopy can quickly and accurately differentiate CCA treated from untreated wood samples in a typical C&D waste stream under actual field conditions. Analysis of the chromium 425.4 nm atomic emission line proved the most reliable metric for CCA detection, which can be combined with analysis of the 422.7 nm calcium emission line for additional signal processing to aid in discrimination of chromium emission not originating from wood, such as nails or metal fasteners. With the proper positioning of the detector above the horizontal conveyor, the LIBS system can accurately analyze wood ranging in size from sheet products to nominally 4 × 4 in. timbers. If a greater range of wood sample sizes is required, the laser could be directed horizontally with the wood placed against a stop as it passes by on the conveyor. This would ensure that the wood was always a fixed distance from the focusing optics, thereby generating a stronger and more reliable plasma emission signal, promoting enhanced precision and accuracy.

ACKNOWLEDGMENTS

The authors would like to acknowledge Gary Jacobi, Naila Hosein, and Helena Solo-Gabriele of the University of Miami and Ken Iida, Jenna Jambeck, and Timothy Townsend of the University of Florida for assistance with the field trials. The authors would like to acknowledge Jim Gabbert and the Meyer and Gabbert C&D Recycling Facility in Sarasota County, Florida, and Gary Bennett of Sarasota County Solid Waste Operations Division, for facilitation and assistance with the field trials. The Florida Department of Environmental Protection, Innovative Recycling Grants Program, in collaboration with Sarasota County Resource Conservation Department, funded this project. T.M.M. would like to acknowledge support from the United States Navy, Civil Engineer Corps.

1. *Wood Preserving Industry Production Statistical Report* (American Wood Preservers Institute, Fairfax, VA, 1996).
2. H. M. Solo-Gabrielle, T. Townsend, J. Penha, T. Tolaymat, and V. Calitu, *Generation, Use, Disposal and Management Options for CCA-Treated Wood*, Final Technical Report #98-1 (Florida Center for Solid and Hazardous Waste Management, Gainesville, FL, 1998).
3. R. S. Atkins and J. E. Fehrs, *Wood Products in the Waste Stream: Characterization and Combustion Emissions*, Energy Authority, Report 92-8, Vol. 1 (New York State Energy Research and Development Authority, New York, 1992).
4. H. C. Holton, *Environ. Health Perspect.* **109**, A274 (2001).
5. *Biocycle* **37**, 39 (1996).
6. H. M. Solo-Gabrielle and T. Townsend, *Waste Manage. Res.* **17**, 378 (1999).
7. S. Klein, T. Stratoudaki, V. Zafirooulos, J. Hildenhagen, K. Dickmann, and T. Lehmkuhl, *Appl. Phys. A* **69**, 441 (1999).
8. R. Barbini, F. Calao, R. Fantoni, A. Palucci, and F. Capitelli, *Appl. Phys. A* **69**, S175 (1999).
9. D. A. Cremers, *Appl. Spectrosc.* **41**, 572 (1987).
10. A. Ciucci, V. Palleschi, S. Rastelli, R. Barbini, F. Colao, R. Fantoni, A. Palucci, S. Ribezzo, and H. J. L. van der Steen, *Appl. Phys. B* **63**, 185 (1996).
11. R. E. Neuhauser, U. Panne, R. Niessner, and P. Wilbring, *Fresenius' J. Anal. Chem.* **364**, 720 (1999).
12. H. Zhang, F. Y. Yueh, and J. P. Singh, *Appl. Opt.* **38**, 1459 (1999).
13. A. Uhl, K. Lobe, and L. Kreuchwig, *Spectrochim. Acta, Part B* **56**, 795 (2001).
14. D. A. Rusak, M. Clara, E. E. Austin, K. Visser, R. Niessner, B. W. Smith, and J. D. Winefordner, *Appl. Spectrosc.* **51**, 1628 (1997).